

## Supplement of

# Flow intermittence prediction using a hybrid hydrological modelling approach: influence of observed intermittence data on the training of a random forest model

Louise Mimeau<sup>1</sup>, Annika Künne<sup>2</sup>, Flora Branger<sup>1</sup>, Sven Kralisch<sup>2</sup>, Alexandre Devers<sup>1</sup>, and Jean-Philippe Vidal<sup>1</sup>

<sup>1</sup>INRAE, UR RiverLy, Centre de Lyon-Villeurbanne, 5 rue de la Doua CS 20244, 69625 Villeurbanne, France

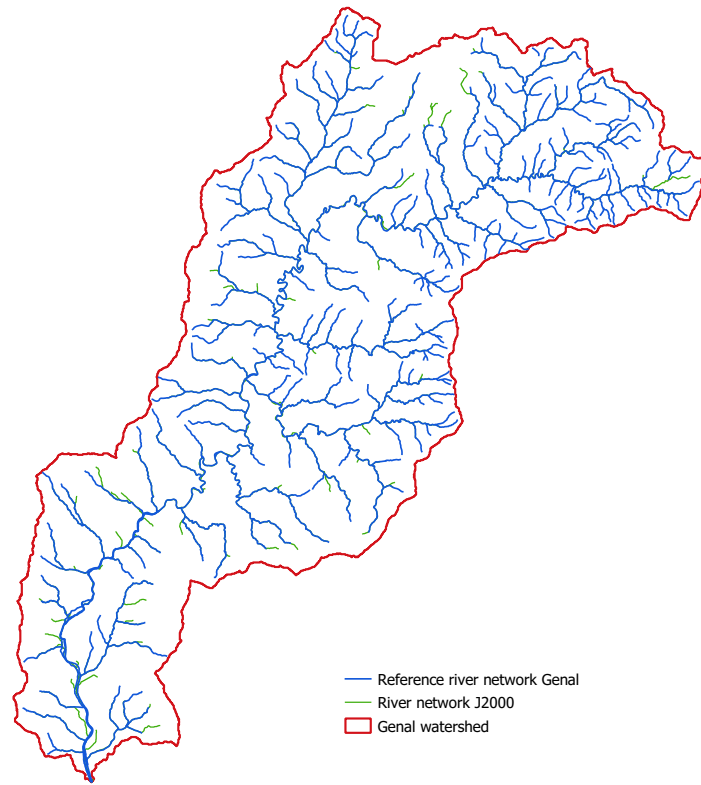
<sup>2</sup>Geographic Information Science Group, Institute of Geography, Friedrich Schiller University Jena, Löbdergraben 32, 07743 Jena, Germany

**Correspondence:** Louise Mimeau (louise.mimeau@inrae.fr)

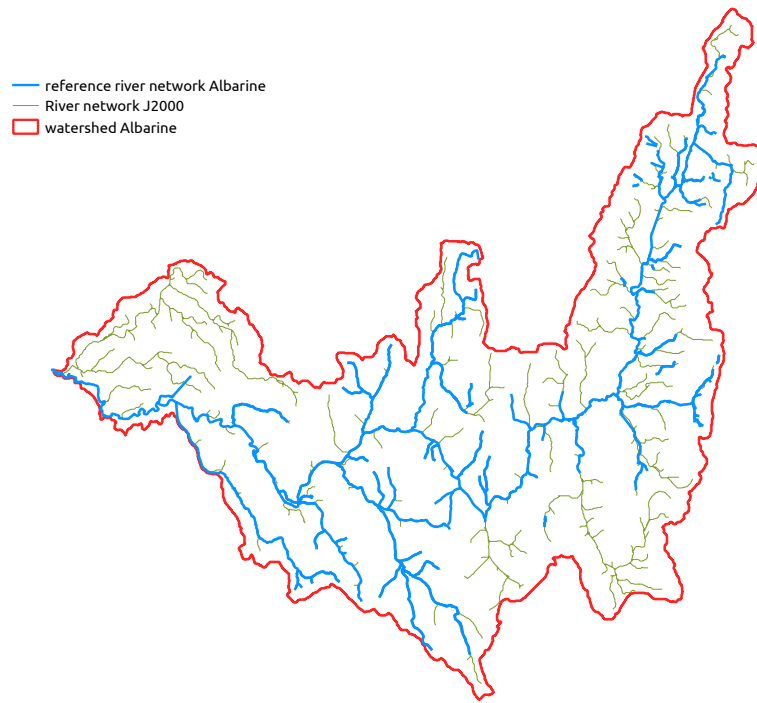
### 1 Adequacy of the JAMS-J2000 river networks with the observed river networks

Figure S.1, S.2 and S.3 show the comparison between the synthetic river networks generated for the hydrological modelling with JAMS-J2000 and reference river networks provided by local DRN teams from the DRYvER project Datry et al. (2021).

- 5 For the Albarine and Lepsämäjoki catchments, the spatial resolution of the generated river networks had to be increased in order to capture all reaches with available observed flow intermittence data.



**Figure S.1.** Generated (green) and observed (blue) river networks for the Genal catchment.



**Figure S.2.** Generated (green) and observed (blue) river networks for the Albarine catchment.

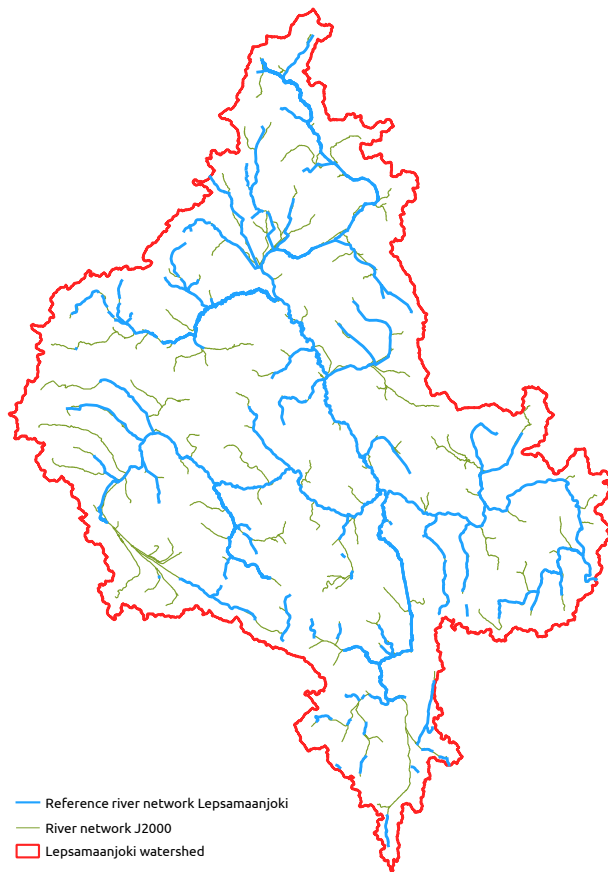


**Figure S.3.** Generated (green) and observed (blue) river networks for the Lepsämäenjoki catchment.

## 2 Calibration of the JAMS-J2000 model

### 2.1 Catchments for JAMS-J2000 calibration

Calibration of the JAMS-J2000 parameters was performed on larger catchments (1500 to 3700 km<sup>2</sup>) corresponding to the  
 10 intermediate-scale basins studied in the DRYvER project (to bridge the gap between the DRN scale and the continental scale).

The larger catchments characteristics are presented in Figure S.4.

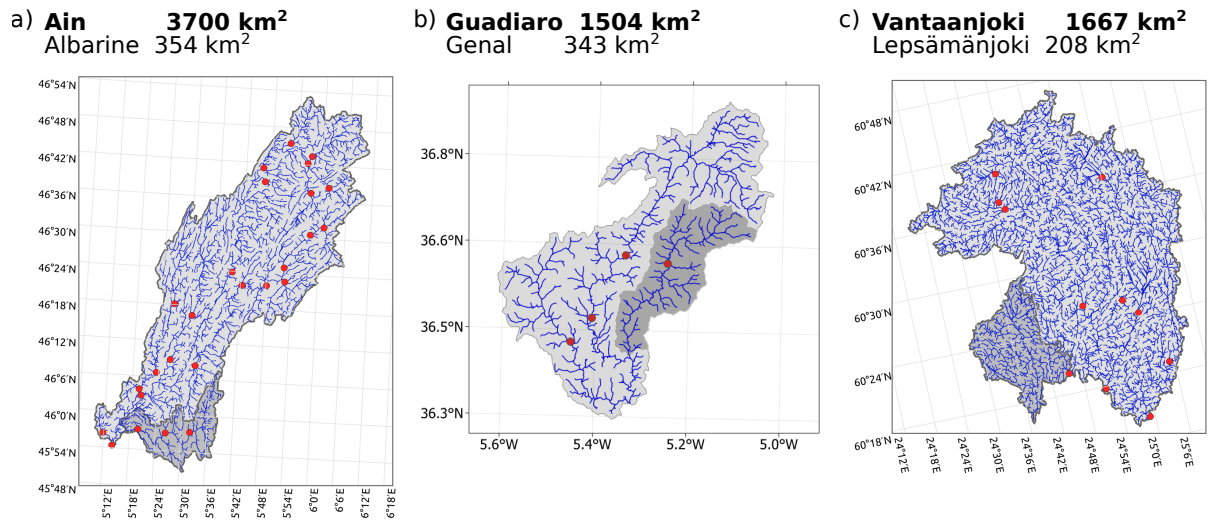


**Figure S.4.** Catchments used for JAMS-J2000 calibration (larger catchments in light grey). Small catchments in dark grey are the catchments used for the flow intermittence modelling. Gauging stations used for the calibration are represented in red. a) French study sites : Ain and Albarine catchments, b) Spanish study sites : Guadiaro and Genal, c) Finnish study sites : Vantaanjoki and Lepsämäenjoki.

## 2.2 Calibration of snow parameters

Snow parameters (Table S.1) were calibrated separately by comparing the simulated snow cover with the catchments' fractional snow cover area from MODIS10A2 datasets using the Kling-Gupta Efficiency (KGE) (Gupta et al., 2009). For that purpose, the catchment fractional snow cover area (fSCA) from the MOD10A2 dataset available at an 8 days resolution (Hall et al., 2007) was used as observed data. For that purpose, MOD10A2 fSCA was downloaded for the period 2000-10-15 to 2021-05-25 and aggregated at the catchment scale. The NSGA-II algorithm (Deb et al., 2002) with 1000 iterations was used for the automatic calibration, and the KGE as an objective function. The model time series were split into a period of initialization (1995 to 2000), a period of calibration (even years from 2000 to 2020), and a period of validation (remaining years from 2000 to 2020).

For the Ain catchment, KGE is respectively equal to 0.81 and 0.74 for the calibration and validation period. For the Vantaanjoki catchment, KGE is respectively equal to 0.80 and 0.74 for the calibration and validation period. Figures S.5 and S.6 show simulated and observed snow cover areas in the Ain and Vantaanjoki catchments. The Guadiaro catchment is not characterized by a regular winter snow cover, and therefore, snow calibration was neglected for this catchment.

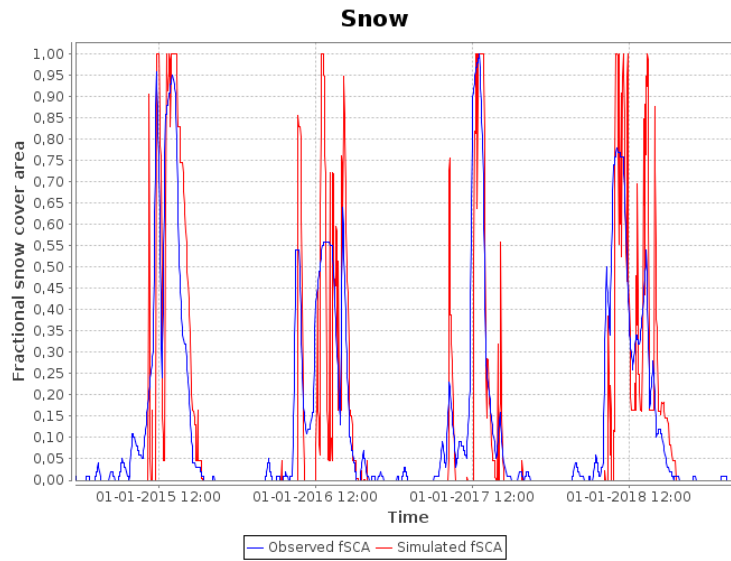


**Figure S.5.** Simulated (red) and observed (blue) snow cover area (fSCA) for the Ain catchment. KGE calibration = 0.81, KGE validation = 0.75

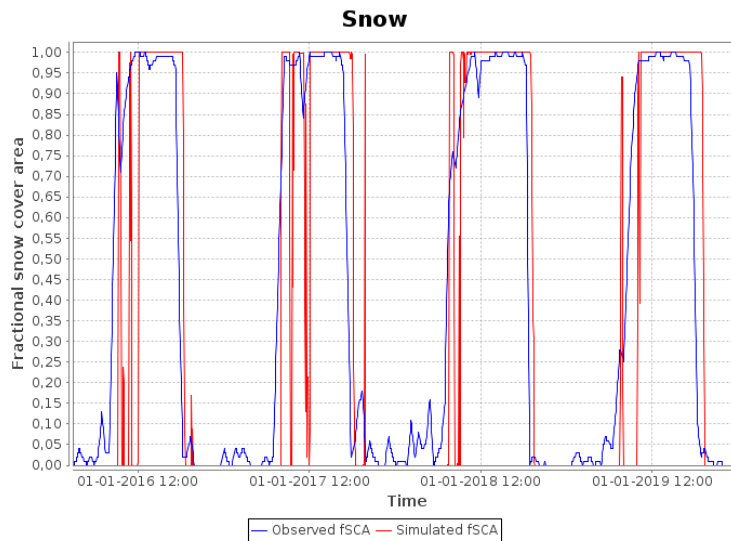


**Figure S.6.** Simulated (red) and observed (blue) snow cover area (fSCA) for the Vantaanjoki catchment. KGE calibration = 0.79, KGE validation = 0.76

25 **2.3 Calibration of discharge**

Measured streamflow available at different gauging stations was used for model calibration and validation. For this purpose, the available streamflow data was split into two periods for calibration and validation (Table S.3). Due to different catchment

30 characteristics, process dynamics, and data availability, the calibration approaches were slightly different for the three catchments. The calibration procedures are therefore presented separately for the Guadiaro catchment on the one hand and for the Ain and Vantaanjoki catchments on the other hand. The list of the calibrated parameters with their calibration range is presented in Tables S.1 and S.2 and all the final parameter values can be found in the JAMS-J2000 model datasets available on request.

| Abbreviation     | Description  | Unit    | Calibration range   |          |
|------------------|--|---------|---------------------|----------|
|                  |  |         | Ain and Vantaanjoki | Guadiaro |
| snow_trans       | Half width of the transition zone rainfall-snowfall  | K       | 0 - 3.5             |          |
| snow_trs         | Threshold temperature for precip phase (the temp. in which 50% of precip fall as snow and 50% as rain) | °C      | 0 - 3               |          |
| t_factor         | Temperature factor for snow melt   | mm*°C-1 | 0 - 8               |          |
| ccf_factor       | Cold content factor  | -       | 0.0001 - 0.01       |          |
| CropCoef_aAF     | Crop coefficient additive adaptation factor  | -       | -0.2 - 0.2          |          |
| CropCoef_mAF     | Crop coefficient multiplicative adaptation factor  | -       | 0.5 - 2             |          |
| FCAdaptation     | Multiplier for field capacity  | -       | 0.5 - 5             | 0.5 - 3  |
| ACAdaptation     | Multiplier for air capacity  | -       | 0 - 3               | 0.5 - 3  |
| soilPolRed       | Polynomic reduction factor for potential evapo-transpiration   | -       | 0 - 10              |          |
| soilMaxInfSnow   | Maximum infiltration for snow covered areas  | mm      | 5 - 200             |          |
| soilMaxInfSummer | Maximum infiltration in summer (Apr - Sep)   | mm      | 5 - 200             |          |
| soilMaxInfWinter | Maximum infiltration in winter (Oct - Mar)   | mm      | 5 - 200             |          |
| soilMaxPerc      | Maximum percolation rate   | mm      | 1 - 20              |          |
| soilLatVertLPS   | LPS lateral-vertical distribution coefficient  | -       | 0 - 10              |          |
| soilOutLPS       | LPS outflow coefficient  | -       | 0 - 10              |          |
| SoilConcRD1      | Recession coefficient for surface runoff   | -       | 1 - 5               | 1 - 10   |
| SoilConcRD2      | Recession coefficient for interflow  | -       | 1 - 10              |          |
| gwRG1RG2dist     | Distribution factor between shallow and deep groundwater aquifer                                       | -       | 0 - 10              |          |
| flowRouteTA      | Flow routing coefficient TA  | -       | 1 - 20              | 1 - 30   |

**Table S.1.** List of the calibrated global parameters and their calibration range

| Abbreviation | Description  | Unit | Calibration range   |  |
|--------------|--|------|---------------------|--|
|              |  |      | Ain and Vantaanjoki | Guadiaro   |
| RG1_max      | Maximum storage capacity of the upper ground-water reservoir | mm   | 10 - 300            | not calibrated                                   |
| RG1_k        | Storage coefficient of the upper ground-water reservoir      | day  | 2 - 30              | 0.3 – 3-times of physically determined parameter |
| RG2_max      | Maximum storage capacity of the lower ground-water reservoir | mm   | 100 - 1500          | not calibrated                                   |
| RG2_k        | Storage coefficient of the lower ground-water reservoir      | day  | 10 - 600            | 0.3 – 3-times of physically determined parameter |

**Table S.2.** List of the calibrated spatially distributed parameters and the calibration range

| DRN           | Initialization period | Calibration period | Validation period |
|---------------|-----------------------|--------------------|-------------------|
| Albarine      | 1990-1995             | 1995-2009          | 2009-2020         |
| Genal         | 1998-2001             | 2001-2004          | 2012-2018         |
| Lepsämäanjoki | 2000-2005             | 2005-2014          | 2014-2020         |

**Table S.3.** Calibration and validation periods. Hydrological years start on the 1<sup>st</sup> of October and end on the 30<sup>th</sup> of September.

### 2.3.1 Model calibration and validation for the Guadiaro catchment

The models' performance of simulating the measured streamflow at multiple gauging stations was evaluated using a semi-automatic calibration method, which utilizes automatic and manual calibration techniques. To assess model performance, different performance criteria were used, which focus on different evaluation criteria, such as low-flow, high flows, and bias (Kundzewicz et al., 2018) (Table S.4).



| Efficiency criteria   | Definition and reason for selection  |
|---|--|
| Nash-Sutcliffe Efficiency (NSE)                             | Multi-objective function, strong focus on simulation of peak flows, widely used  |
| Logarithmic Nash-Sutcliffe Efficiency (NSE <sub>log</sub> ) | Like NSE, but logarithm focuses on the representation of simulation of low flows |
| Relative Volume Error (pBias)                               | Representing overall under or overestimation                                     |
| Kling-Gupta-Efficiency (KGE)                                | multi-objective function, representing bias, correlation, and flow variability   |

**Table S.4.** Efficiency criteria used for automatic model calibration and performance evaluation (Gupta et al., 2009)

Overall, 15 global model parameters were calibrated, which showed a moderate to high sensitivity on processes related to infiltration, evapotranspiration, percolation, soil, groundwater, and runoff routing (Tables S.1 and S.2). Besides, hydrogeological parameters influencing the recession of the water from shallow and deep groundwater aquifers were calibrated in a spatially distributed manner. For the automatic optimization, the multi-objective, non-dominated sorting genetic search algorithm NSGA-II was applied (Deb et al., 2002). Here, the three performance criteria NSE, NSE<sub>log</sub> and pBias at different gauging stations were used in 5000 iterations to optimize the 15 parameters and hence, simulated streamflow in the Genal DRN. Additionally, the process was repeated for different spatially distributed hydrogeology parameter sets addressing the varying groundwater recession from shallow and deep groundwater aquifers. This resulted in several pareto-optimal model solutions, which still inherited strong differences of hydrological process patterns, considering, for example, the overland flow or groundwater contribution to the overall runoff. Even though statistical measures have the advantage to objectively classify model performance and allow comparison across different models, they do not substitute visual interpretation of simulated and observed hydrographs and interpretation of process dynamics by domain experts (Legates and McCabe Jr, 1999; Moriasi et al., 2007). Therefore, the models were manually calibrated in a second step to fine-tune the results of the automated calibration procedure. The focus here was particularly on the representation of the runoff recession and groundwater contribution. Besides, due to the modeling of flow intermittence, the performance of modeling low flows was weighted higher than the model's ability to simulate high flows accurately. Further, when selecting the final parameter sets for the DRN, sets showing higher performance at the smaller basin were given preference over sets showing higher performance at the larger basin. During calibration, the following hydrological characteristics were taken into account:

1. runoff components (Hortonian and Hewlettian runoff, subsurface flow from soil and upper groundwater zones as well as baseflow), precipitation, actual evapotranspiration, and soil saturation;
2. seasonal and annual water balances;
3. spatially distributed processes at the HRU level: runoff generation, interflow, soil water balancing, evapotranspiration, and groundwater recharge.

Finally, from all pareto-optimal solutions identified through automatic and manual calibration, the most plausible model in terms of process representation according to the observed data and the knowledge about environmental characteristics was selected.

Figures S.7 and S.8 show the performance of the JAMS-J2000 model in the Guadiaro catchment.

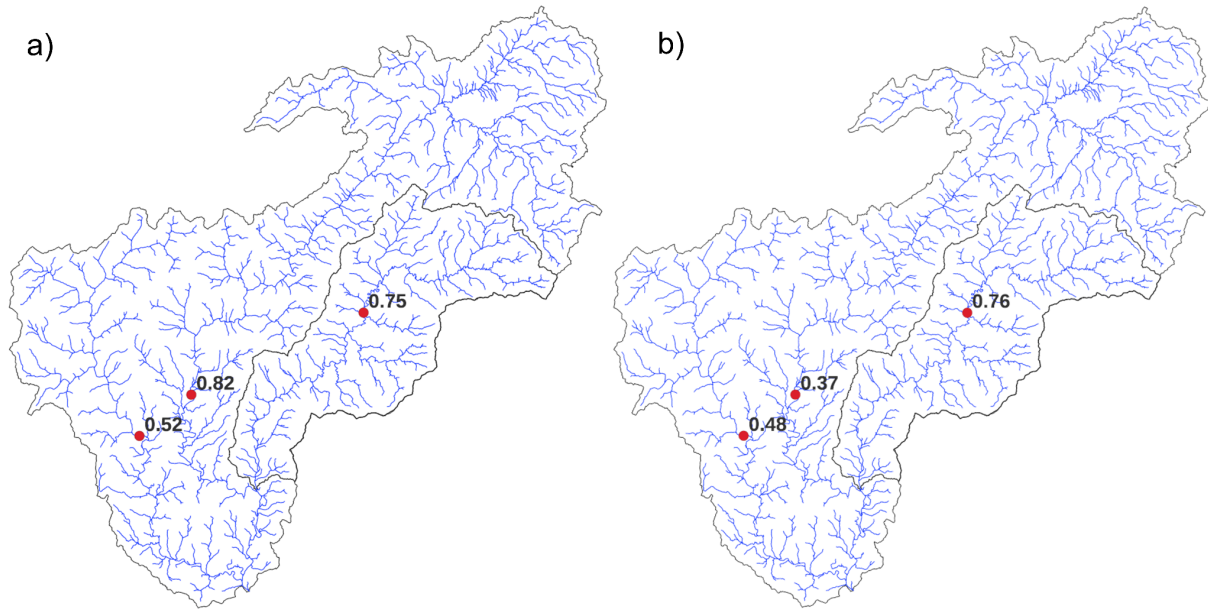


**Figure S.7.** KGE for the a) calibration period (2002 - 2012; Genal: 2001 - 2004) and b) the validation period (2012 - 2018) for the Guadiaro catchment

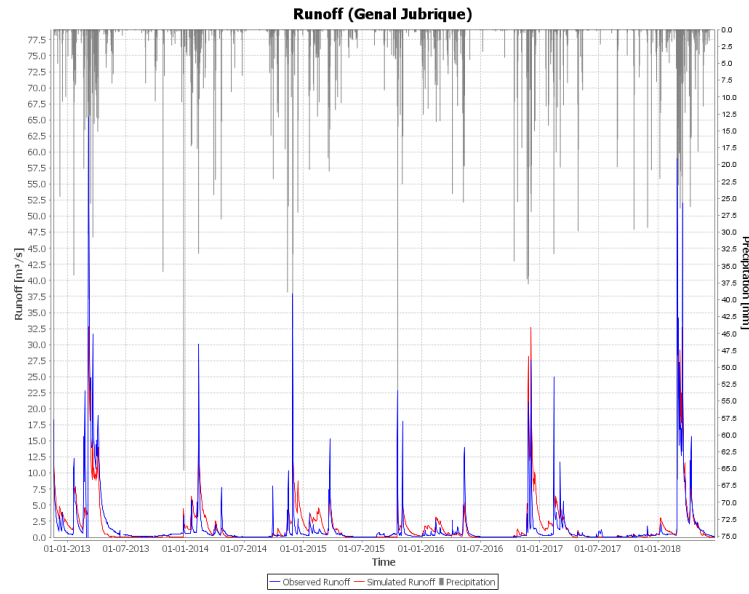


**Figure S.8.** Simulated (red) and observed (blue) discharge at the Jubrique gauging station (in the Genal catchment). KGE calibration = 0.75, KGE validation = 0.76

### 65 2.3.2 Model calibration and validation for the Ain and Vantaanjoki catchments

The calibration for the Ain, Fekete, and Vantaanjoki catchments also uses a multi-stations and multi-objectives approach, but using a different method. 15 global parameters related to evapotranspiration, infiltration in the soil layer, and percolation to the groundwater layer, (Table S.1) as well as 4 spatially distributed parameters related to the groundwater reservoirs (Table S.2), are calibrated. The calibration and validation periods (Table S.4) were selected based on the availability of the observed discharge data in the different river basins. In a first step, the Latin Hyper Cube Sampling (LHS) is used to generate 5000 model runs for each pilot river basin (the calibration ranges are provided in Tables S.1 and S.2). Then the calibrated set of parameters is selected among the 5000 parameters sets so that the model performs best on (i) a multi-objective function (*MOF*) representing KGE, low-flows (10<sup>th</sup> percentile  $Q_{10}$ ), and mean annual outflow ( $Q_{yr}$ ), (ii) all the stations. The *MOF* function is computed for all stations and all parameter sets (Eq. 1), then a weighted average over the stations is calculated to prioritize the stations located at the outlets of the large and small river basins ( $Ref_1$ ) and the other stations located in the small river basin ( $Ref_2$ ) (Eq. 2) (other stations located in the large catchment are referred as  $Ref_3$ ). The final calibrated set of parameters is selected among the model runs leading to the lowest  $MOF_{allstations}$ .

$$MOF = 0.6 * (1 - KGE) + \frac{0.2 * |Q_{10_{sim}} - Q_{10_{obs}}|}{Q_{10_{obs}}} + \frac{0.2 * |Q_{yr_{sim}} - Q_{yr_{obs}}|}{Q_{yr_{obs}}} \quad (1)$$

$$MOF = \frac{w_{Ref_1} \sum_{i \in Ref_1} MOF_i + w_{Ref_2} \sum_{j \in Ref_2} MOF_j + w_{Ref_3} \sum_{k \in Ref_3} MOF_k}{\sum_{i \in Ref_1} w_{Ref_1} + \sum_{j \in Ref_2} w_{Ref_2} + \sum_{k \in Ref_3} w_{Ref_3}} \quad (2)$$

80  $\text{with } w_{Ref_1} = 5, w_{Ref_2} = 2, w_{Ref_3} = 1$

The Ain catchment is characterized by karstic areas which have a strong impact on the hydrological response of the sub-catchments. As the JAMS-J2000 model does not represent the karst-related processes, a correction factor  $k$  was applied to the observed discharges at the gauges before comparison with simulated discharges to consider water input or water losses in sub-catchments through the karstic network (Eq. 3).

85  $k = \frac{P - ET_{act} - Q}{P - ET_{act}} \quad (3)$

with  $P$  the observed mean annual precipitation in mm (from the Safran reanalysis; Vidal et al. (2010)),  $ET_{act}$  the mean annual actual evapotranspiration simulated with JAMS-J2000 in mm (forced with Safran reanalysis as climate input data), and  $Q$  the observed mean annual outflow in mm.

Figures S.9 and S.10 show the performance of the JAMS-J2000 model in the Ain catchment.

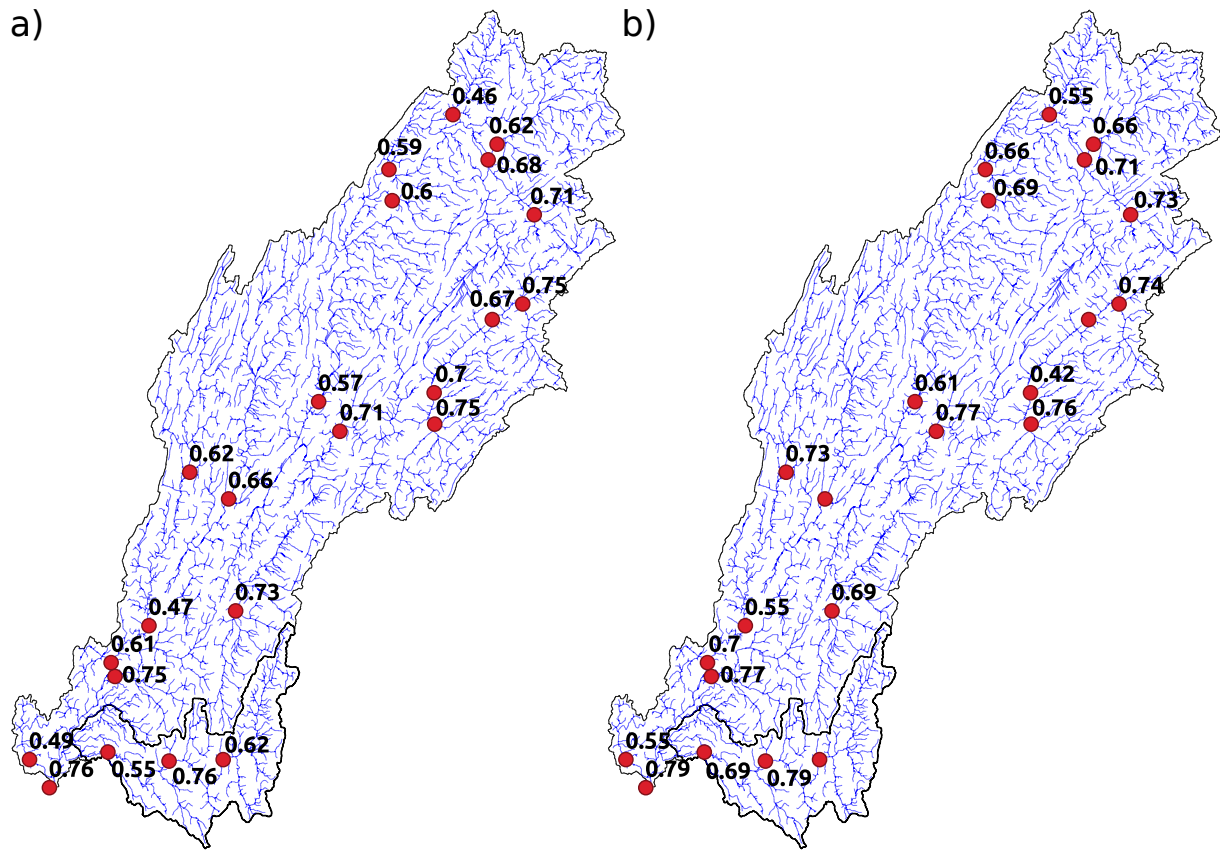


**Figure S.9.** KGE for the a) calibration period (1995-2009) and b) the validation period (2009-2019) for the Ain catchment. Missing values during the validation period are due to the shutdown of gauging stations

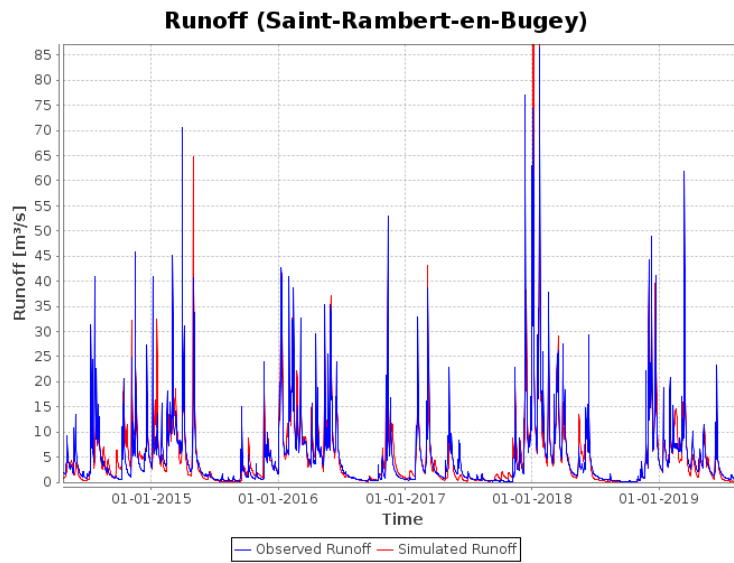


**Figure S.10.** Simulated (red) and observed (blue) discharge at the Saint-Rambert station (in the Albarine catchment) for the validation period. KGE calibration = 0.76, KGE validation = 0.79

90

Figures S.11 and S.12 show the performance of the JAMS-J2000 model in the Vantaanjoki catchment.

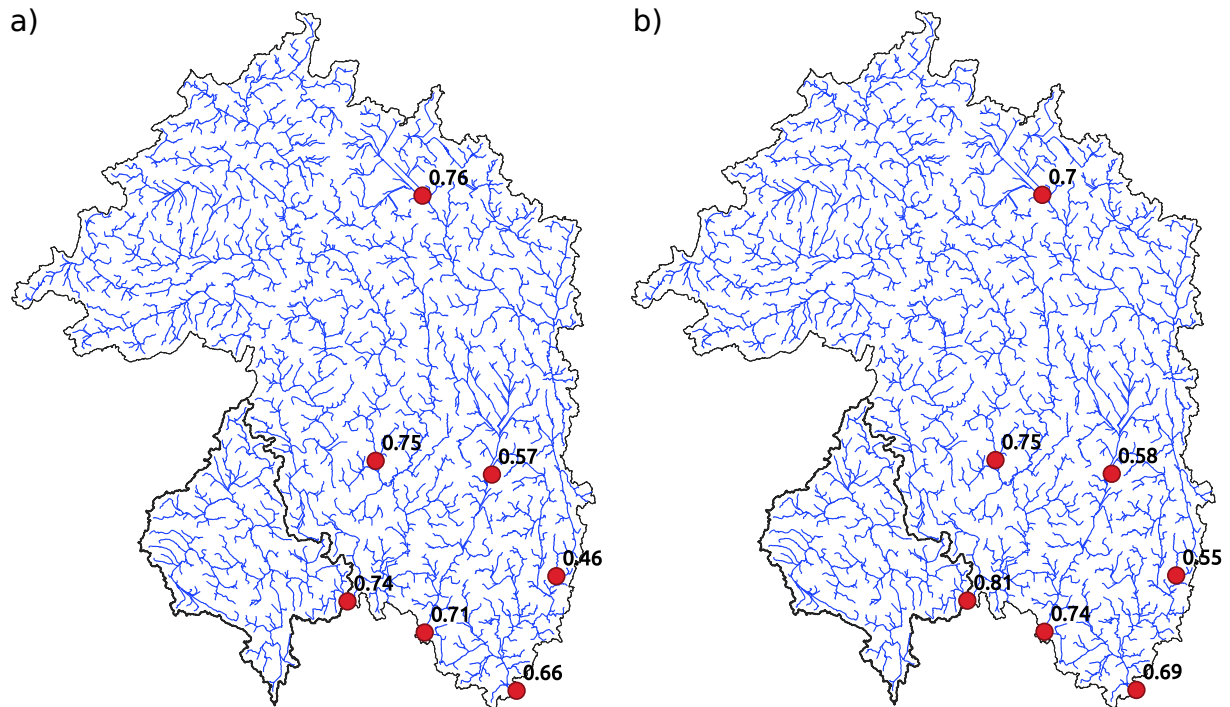


**Figure S.11.** KGE for the a) calibration period (2005-2014) and b) the validation period (2014-2020) for the Vantaanjoki catchment

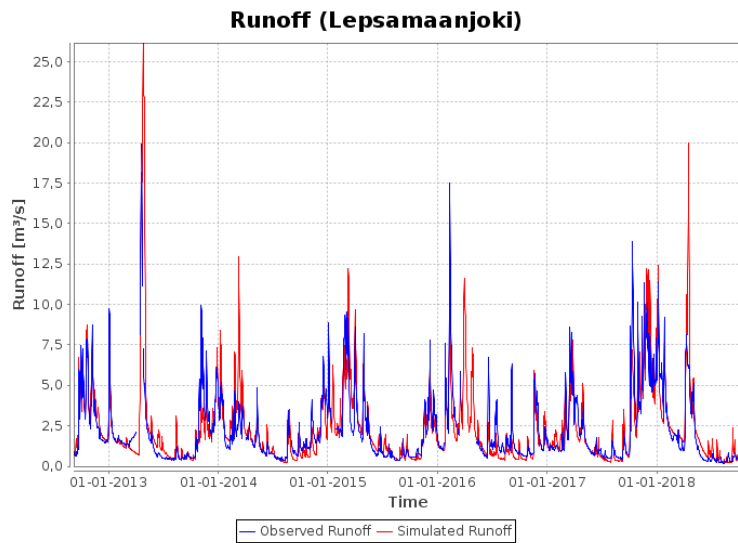


**Figure S.12.** Simulated (red) and observed (blue) discharge at the Lepsämänjoki station for the validation period. KGE calibration = 0.74, KGE validation = 0.81

### 3 Validation of the simulated spatial flow intermittence pattern in the Albarine and Genal DRNs

Some classification of the reaches flow regime (permanent or intermittent) were provided for the Albarine and Genal DRN by local teams based on their observations. Figures S.13 and S.14 show the comparison between the simulated spatial pattern of flow intermittence in the Albarine and Genal DRNs with the observed flow regimes in the river networks.

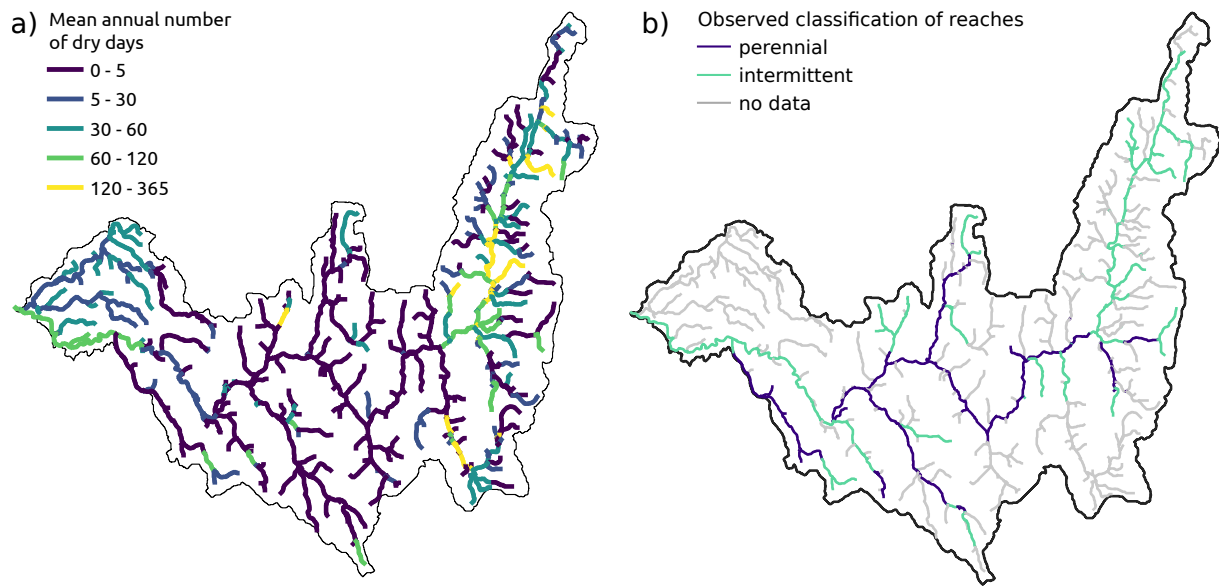


**Figure S.13.** a) Mean annual number of days with a dry condition predicted in the Albarine DRN with the flow intermittence model, b) classification of the reaches (perennial or intermittent) provided by the DRN local experts based on observations.

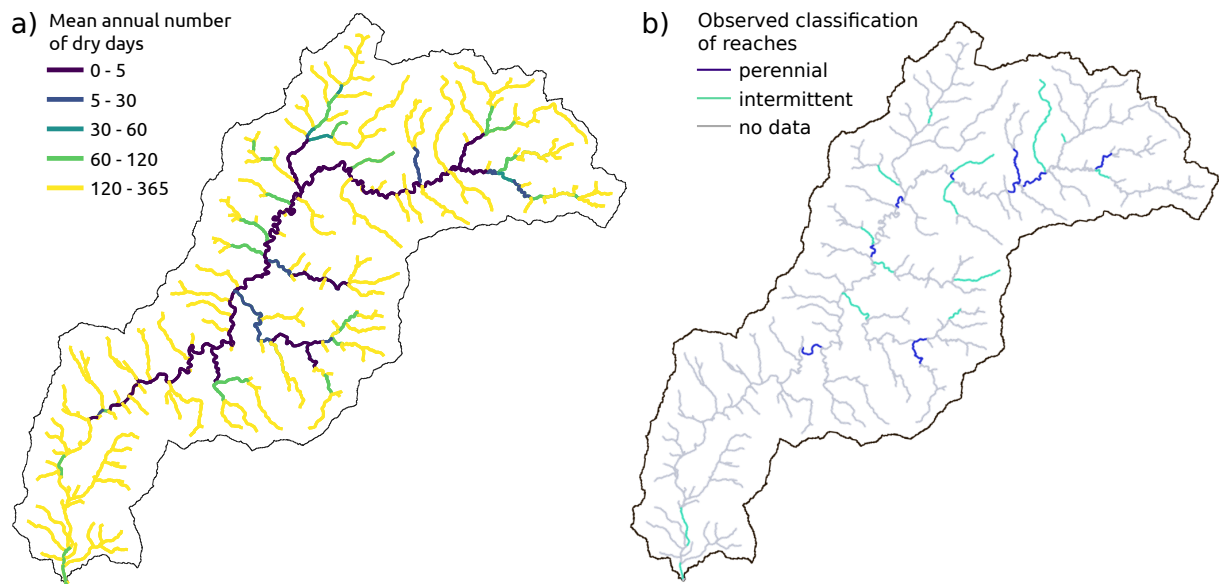


**Figure S.14.** a) Mean annual number of days with a dry condition predicted in the Genal DRN with the flow intermittence model, b) classification of the reaches (perennial or intermittent) provided by the DRN local experts based on observations.



## 95 References

- Datry, T., Allen, D., Argelich, R., Barquin, J., Bonada, N., Boulton, A., Branger, F., Cai, Y., Cañedo-Argüelles, M., Cid, N., et al.: Securing Biodiversity, Functional Integrity, and Ecosystem Services in Drying River Networks (DRYvER), *Research Ideas and Outcomes*, 7, e77750, <https://doi.org/10.3897/rio.7.e77750>, 2021.
- Deb, K., Pratap, A., Agarwal, S., and Meyarivan, T.: A fast and elitist multiobjective genetic algorithm: NSGA-II, *IEEE transactions on evolutionary computation*, 6, 182–197, <https://doi.org/10.1109/4235.996017>, 2002.
- 100 Gupta, H. V., Kling, H., Yilmaz, K. K., and Martinez, G. F.: Decomposition of the mean squared error and NSE performance criteria: Implications for improving hydrological modelling, *Journal of hydrology*, 377, 80–91, <https://doi.org/10.1016/j.jhydrol.2009.08.003>, 2009.
- Hall, D., Riggs, G., and Salomonson, V.: MODIS/Terra Snow Cover 8-Day L3 Global 500 m Grid V005. National Snow and Ice Data Centre, Digital media, Boulder, 2007.
- 105 Kundzewicz, Z., Krysanova, V., Benestad, R., Hov, Ø., Piniewski, M., and Otto, I.: Uncertainty in climate change impacts on water resources, *Environmental Science & Policy*, 79, 1–8, <https://doi.org/10.1016/j.envsci.2017.10.008>, 2018.
- Legates, D. R. and McCabe Jr, G. J.: Evaluating the use of “goodness-of-fit” measures in hydrologic and hydroclimatic model validation, *Water resources research*, 35, 233–241, <https://doi.org/10.1029/1998WR900018>, 1999.
- Moriasi, D. N., Arnold, J. G., Van Liew, M. W., Bingner, R. L., Harmel, R. D., and Veith, T. L.: Model evaluation guidelines for systematic  
110 quantification of accuracy in watershed simulations, *Transactions of the ASABE*, 50, 885–900, <https://doi.org/10.13031/2013.23153>, 2007.
- Vidal, J.-P., Martin, E., Franchistéguy, L., Baillon, M., and Soubeyroux, J.-M.: A 50-year high-resolution atmospheric reanalysis over France with the Safran system, *International Journal of Climatology*, 30, 1627–1644, <https://doi.org/10.1002/joc.2003>, 2010.